Available online at www.sciencedirect.com
SCIENCE DIRECT®
Journal of Solid State Chemistry 178 (2005) 1705–1711
JOURNAL OF SOLID STATE CHEMISTRY
www.elsevier.com/locate/jssc

Oxygen nonstoichiometry and valence of copper in the Cu-1222 superconductor

M. Karppinen[a,*], M. Arai[a], J.M. Lee[b], T.S. Chan[c], Y. Morita[a], J.M. Chen[b], R.S. Liu[c], H. Yamauchi[a]

[a]*Materials and Structures Laboratory, Tokyo Institute of Technology, Yokohama 226-8503, Japan*
[b]*National Synchrotron Radiation Research Center (NSRRC), Hsinchu, Taiwan, ROC*
[c]*Department of Chemistry, National Taiwan University, Taipei, Taiwan, ROC*

Received 15 December 2004; received in revised form 2 March 2005; accepted 18 March 2005

Abstract

Essentially single-phase $Cu(Ba_{0.67}Eu_{0.33})_2(Ce_{0.33}Eu_{0.67})_2Cu_2O_{9\pm\delta}$ samples of the Cu-1222 phase with a fluorite-structured (Ce,Eu)–O_2–(Ce,Eu) block between the superconductive CuO_2 planes were synthesized in O_2 atmosphere to exhibit superconductivity with T_c around 25 K. Wide-range tuning of oxygen content and thereby the overall hole-doping level of the phase was found possible through (i) temperature-controlled oxygen-depletion (TCOD) annealing carried out in a thermobalance in N_2 at various temperatures (for reduction), and (ii) high-pressure oxygenation (HPO) treatments carried out in a cubic-anvil-type high-pressure apparatus in the presence of various amounts of Ag_2O_2 as an excess oxygen source (for oxidation). For the HPO samples a record-high T_c value of 62 K was achieved. On the other hand, deoxygenation to the oxygen content less than $9\pm\delta\approx 8.9$ was found to kill superconductivity. The degree of hole doping (both in overall and for the CuO_2 plane and $CuO_{1\pm\delta}$ charge reservoir separately) in the samples is discussed on the bases of Cu *L*-edge and O *K*-edge XANES data.

Keywords: Cu valence; XANES spectroscopy

1. Introduction

The first high-T_c superconductive copper oxide to contain a fluorite-structured (Ce,*R*)–$[O_2$-(Ce,*R*)$]_{s-1}$ block (*R* = rare-earth element; oxidation states Ce^{IV} and R^{III} expected) between superconductive CuO_2 planes was discovered in the Ce–Nd–Sr–Cu–O system in 1988 by Akimitsu et al. [1,2]. The so-called T^* structure of this $(Ce,Nd,Sr)_2CuO_4$ compound is a 1:1 piling of La_2CuO_4-type (T structure [3,4]) and Nd_2CuO_4-type (T' structure [5]) slabs with a layer sequence of $[(Nd,Sr)O–(Nd,Sr)O]_{RS}$–$[CuO_2]_P$–[(Ce,*R*)–O_2–(Ce,*R*)$]_F$–$[CuO_2]_P$, where RS (rock-salt), P (perovskite) or F (fluorite) refers to the structure type of the corresponding layer/block. Soon after Tokura et al. [6] found the second copper-oxide superconductor with F-type layers, i.e., $(Ce,Nd)_2CuO_4$ of the bare T' structure. Then, $Cu(Ba,R)_2(Ce,R)_2Cu_2O_{9\pm\delta}$ with a layer sequence of $[(Ba,R)O]_{RS}$–$[CuO_{1\pm\delta}]_P$–$[(Ba,R)O]_{RS}$–$[CuO_2]_P$–[(Ce,*R*)–O_2–(Ce,*R*)$]_F$–$[CuO_2]_P$ became the third superconductor having the (Ce,*R*)–$[O_2$–(Ce,*R*)$]_{s-1}$ block [7]. With later discoveries it has turned out that all these three phases are members of a larger group of multi-layered copper oxides that contain F-type layers between two adjacent CuO_2 planes and an $(MO_{1\pm\delta/m})_m$ (*M* = Cu, Bi, Pb, Tl, Hg, etc.; $0\leqslant m\leqslant 3$) "charge reservoir" between two RS-type *A*O (*A* = Sr, Ba, *R*, etc.) layers, i.e., $[AO]_{RS}$–$[(MO_{1\pm\delta/m})_m]_{P/RS}$–$[AO]_{RS}$–$[CuO_2]_P$–[(Ce,*R*)–$\{O_2$–(Ce,*R*)$\}_{s-1}]_F$–$[CuO_2]_P$. Such a phase obeys the general stoichiometry expression of $M_mA_{2k}(Ce,R)_sCu_{1+k}O_{m+4k+2s\pm\delta}$ or $M{-}m(2k)s(1+k)$ in short [8,9].

*Corresponding author. Fax: +81 45 924 5365.
E-mail address: karppinen@msl.titech.ac.jp (M. Karppinen).

0022-4596/$ - see front matter © 2005 Elsevier Inc. All rights reserved.
doi:10.1016/j.jssc.2005.03.026

Here one should recognize that many of the most common high-T_c superconductors are composed of P- and RS-type layers only, to obey a layer sequence of $[AO]_{RS}$–$[(MO_{1\pm\delta/m})_m]_{P/RS}$–$[AO]_{RS}$–$[CuO_2$–$(Q$–$CuO_2)_{n-1}]_P$ (Q = Ca, R, etc.) and a stoichiometry of $M_mA_2Q_{n-1}Cu_nO_{m+2+2n\pm\delta}$ or $M{-}m2(n{-}1)n$. We classify these latter phases as members of "Category-A", while those containing the F-structured block are defined to belong to "Category-B" [9,10].

For Category-A phases, the amount of accumulated experimental data is huge and accordingly various relations among the layer piling, crystallographic fine-structure, oxygen nonstoichiometry, doping and superconductivity characteristics have been uncovered [9,11], whereas Category-B phases are much less investigated and therefore poorly understood. The $s = 2$ member of the Category-B homologous series [12] of Cu-12s2 is an interesting target for deeper oxygen nonstoichiometry and hole doping studies: the first member of the same series, i.e., Cu-1212 [9,13], is nothing but the prototype superconductor, $CuBa_2RCu_2O_{7\pm\delta}$ ("R-123") [14], whereas the third member, obtained in the single-phase form for $(Cu_{0.75}Mo_{0.25})Sr_2(Ce_{0.67}Y_{0.33})_3Cu_2O_{11\pm\delta}$, very recently turned out to be the first "triple-fluorite-layer" superconductor [15]. The first samples of the Cu-1222 ($s = 2$) phase by Sawa et al. [7] were synthesized in O_2 with the stoichiometry of $Cu(Ba,R)_2(Ce,R)_2Cu_2O_{9\pm\delta}$. Among the samples, the highest T_c of 43 K was due to the R = Eu sample after post-annealing under elevated O_2 pressures. The role of the trivalent R substituent at the A (= Ba) site was to stabilize the structure. The Cu-1222 structure is also stabilized for A = Sr by substituting the charge-reservoir Cu partially by higher-valent elements, e.g., $(Cu,Mo)Sr_2(Ce,Y)_2Cu_2O_{9\pm\delta}$ [15,16]. With Sr at the A site, the Cu-1222 structure is formed even without structure-stabilizing substituents, i.e., $CuSr_2(Ce,Y)_2Cu_2O_{9+\delta}$, though only through synthesis under high O_2 pressures [17].

Here we selected the original cation composition, $Cu(Ba_{0.67}Eu_{0.33})_2(Ce_{0.33}Eu_{0.67})_2Cu_2O_{9\pm\delta}$ [7], of the Cu-1222 phase for a systematic oxygen content/valence tuning study. By taking advantage of both deoxygenation (in N_2) and oxygenation (under high O_2 pressures) annealings the hole-doping level of the phase could be continuously controlled from a nondoped (nonsuperconductive) state to a slightly overdoped state. Accordingly, the value of T_c increased up to 62 K, to clearly exceed any of the values previously reported for various Cu-1222 structured compounds.

2. Experimental

The $Cu(Ba_{0.67}Eu_{0.33})_2(Ce_{0.33}Eu_{0.67})_2Cu_2O_{9\pm\delta}$ master sample was prepared by solid-state reaction from a powder mixture of CuO, $BaCO_3$, Eu_2O_3 and CeO_2 with the ratio, Eu:Ba:Ce:Cu = 6:4:2:9. Following the recipe given in the original work by Sawa et al. [7] two heat treatments (for a pelletized powder with an intermediate grinding) were employed, both at 1020 °C for 15 h in flowing O_2 gas. After the second heat treatment the sample was furnace-cooled in O_2 and powdered. Portions of this as-O_2-synthesized powder (henceforth called AS sample) were subjected to different post-annealing treatments in order to either increase or decrease the oxygen content. For oxygenation, the sample was mixed with 12.5–200 mol% Ag_2O_2, loaded in a gold capsule and annealed in a cubic-anvil-type ultra-high-pressure apparatus at 5 GPa and 500 °C for 30 min. Under these conditions Ag_2O_2 functions as an efficient oxygen source upon decomposing to Ag_2O and/or Ag metal [15,18]. The thus obtained high-pressure oxygenated samples are henceforth called HPO samples with a suffix that indicates the amount (in mol%) of Ag_2O_2 used, e.g., HPO:100 for 100 mol% Ag_2O_2. Deoxygenation was carried out by employing our temperature-controlled oxygen-depletion (TCOD [9,18]) technique by annealing a powder sample (ca. 100 mg) in flowing N_2 gas at a prefixed temperature of 300, 400 or 500 °C in a thermobalance (Perkin Elmer: Pyris 1). The heating rate was 20 °C/min. At the final temperature the sample was kept isothermally until the weight loss of the sample saturated (ca. 24 h), and then cooled with a rate of 20 °C/min back to room temperature. These deoxygenated samples are called TCOD-300, TCOD-400 and TCOD-500.

All the samples were characterized by powder X-ray diffraction (XRD; Rigaku: RINT2550VK/U; Cu$K\alpha$ radiation) for phase purity and lattice parameters. Oxygen contents of the AS and TCOD samples were determined by the iodometric titration method that detects the total amount of high-valent metal species, $Cu^{II/III}$ and Ce^{IV} [19]. Superconductivity properties were evaluated from both resistivity (ρ) and magnetic susceptibility (χ) measurements. The former measurements were carried out using a four-probe apparatus and the latter using a SQUID magnetometer (Quantum Design: MPMS-XL) under an applied magnetic field of 10 Oe in both zero-field-cooled (ZFC) and field-cooled (FC) modes. For the superconductive samples the value of T_c was defined at the onset temperature of the diamagnetic signal.

For the estimation of the average valence state of copper X-ray absorption near-edge structure (XANES) spectra were collected for the samples at the Cu $L_{2,3}$ edge. In addition, for the AS and TCOD samples O K-edge XANES spectra were collected for the layer-specific hole concentrations. The XANES experiments were performed at the 6-m HSGM beam-line of NSRRC in Hsinchu (Taiwan) in X-ray fluorescence-yield mode. The spectra were corrected for the energy-dependent incident photon intensity and self-absorption

effects, and normalized to the tabulated standard absorption cross-sections in the energy range of 1000–1020 eV for the Cu $L_{2,3}$ edge and 600–620 eV for the O K edge; details were as those given in Ref. [20].

3. Results and discussion

From X-ray diffraction observation the synthesized $Cu(Ba_{0.67}Eu_{0.33})_2(Ce_{0.33}Eu_{0.67})_2Cu_2O_{9\pm\delta}$ samples were found to be of high quality, all the prominent diffraction peaks detected being due to the Cu-1222 phase. In Fig. 1, diffraction patterns for the TCOD-400, AS and HPO:50 samples are shown. The only undesirable impurity peak, seen about 28.55°, was assigned to a trace of CeO_2 impurity. The amount of the CeO_2 trace remained essentially constant for the entire sample series. Besides the CeO_2 trace, the HPO samples should contain decomposition residue(s) of Ag_2O_2, i.e., Ag_2O and/or Ag, as a natural consequence of the synthesis procedure. Apparently the Ag-containing phases are of rather low crystallinity, since even the main diffraction peaks due to Ag_2O/Ag were hardly visible. For all the samples the diffraction peaks due to the Cu-1222 phase were readily indexed in a body-centered tetragonal symmetry (space group $I4/mmm$ [7]). Lattice parameters refined from the data are given in Table 1. From Table 1, we conclude that deoxygenation/oxygenation slightly increases/decreases the parameter c, whereas the parameter a remains constant. Parallel trends were observed for the $s = 3$ member of the Cu-12s2 homologous series upon similar HPO treatments [15].

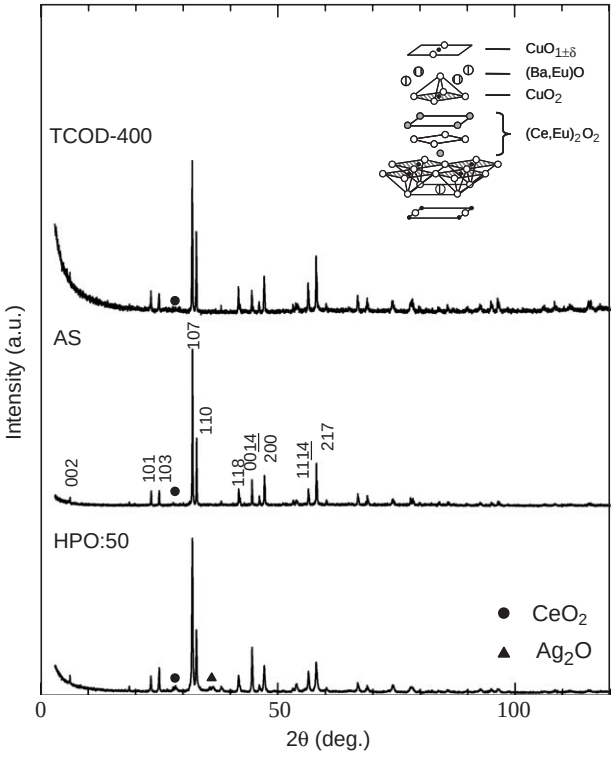

Fig. 1. X-ray powder diffraction patterns for the TCOD-400, AS and HPO:50 samples of $Cu(Ba_{0.67}Eu_{0.33})_2(Ce_{0.33}Eu_{0.67})_2Cu_2O_{9\pm\delta}$. Indices are for the Cu-1222 structure ($I4/mmm$).

The values for the oxygen content, $9\pm\delta$, and the corresponding (nominal average) Cu valence, $V(Cu)_{tit}$, as obtained for the AS and TCOD samples from iodometric titrations are given in Table 1. Note that for the HPO samples, no attempts to employ the iodometric titration method for oxygen-content determination were made due to the presence of nondefined amounts of Ag_2O and/or Ag. For the AS sample, the precise oxygen content, $9\pm\delta$, was determined at 9.02. This is compatible with a $CuO_{1\pm\delta}$ charge-reservoir composition of $1\pm\delta = 1.02$, if all other layers are assumed to be stoichiometric in terms of oxygen [21]. A similar situation with $1\pm\delta$ being larger than unity is seen also for the Cu-1212 phase when the A site is co-occupied by divalent Ba and trivalent R [22,23]. Deoxygenation of the AS sample by means of TCOD annealing decreased the $9\pm\delta$ value from 9.02 to 8.96 for TCOD-300, 8.90 for TCOD-400 and 8.82 for

Table 1
Experimental data for the $Cu(Ba_{0.67}Eu_{0.33})_2(Ce_{0.33}Eu_{0.67})_2Cu_2O_{9\pm\delta}$ (Cu-1222) samples: oxygen content $9\pm\delta$, lattice parameters, a and c, the T_c value and the superconductivity volume fraction, average nominal Cu valence as estimated from the redox titration data [$V(Cu)_{tit}$] and from the Cu L_3-edge XANES data [$V(Cu)_{XAS}$] (see the text for definition), and the individual CuO_2-plane and $CuO_{1\pm\delta}$-charge-reservoir hole concentrations, $p(CuO_2)_{XAS}$ and $p(CuO_{1\pm\delta})_{XAS}$, as estimated on the basis of the O K-edge XANES data (see the text for definition)

Sample	a (Å)	c (Å)	$9\pm\delta$	$V(Cu)_{tit}$	$V(Cu)_{XAS}$	$p(CuO_2)_{XAS}$	$p(CuO_{1\pm\delta})_{XAS}$	T_c (K) (vol. fraction)
TCOD-500	3.86	28.50	8.82	2.11	2.04	0.06	0.00	< 4
TCOD-400	3.86	28.49	8.90	2.16	2.05	0.07	0.01	< 4
TCOD-300	3.86	28.49	8.96	2.20	2.10	0.10	0.02	15 (12%)
AS	3.86	28.48	9.02	2.24	2.12	0.10	0.03	25 (29%)
HPO-12.5	3.86	28.47	—	—	—	—	—	42 (24%)
HPO:25	3.86	28.46	—	—	—	—	—	55 (31%)
HPO:50	3.86	28.46	—	—	2.20	—	—	62 (51%)
HPO:100	3.86	28.48	—	—	2.24	—	—	62 (59%)
HPO:150	3.86	28.47	—	—	2.30	—	—	58 (35%)
HPO:200	3.86	28.46	—	—	2.33	—	—	58 (150%)

TCOD-500, according to iodometric titrations. Reading the oxygen contents for the TCOD annealed samples directly from the corresponding thermogravimetric (TG) curves (Fig. 2) gives values of 8.94, 8.89 and 8.82, respectively. Hence the TG data corroborate the iodometric titration results, though it should be recognized that the TG curves for the TCOD annealings reveal no absolute but relative oxygen-content values only. From preliminary experiments it was known that heating the $Cu(Ba_{0.67}Eu_{0.33})_2(Ce_{0.33}Eu_{0.67})_2Cu_2O_{9\pm\delta}$ samples in N_2 to temperatures higher than 500 °C ended up with gradual decomposition of the Cu-1222 phase. Hence, the $9\pm\delta$ value of 8.82 determined here for the TCOD-500 sample is believed to be close to the lowest level of oxygen content yet tolerated by the Cu-1222 structure (at the cation stoichiometry of $Cu(Ba_{0.67}Eu_{0.33})_2(Ce_{0.33}Eu_{0.67})_2Cu_2O_{9\pm\delta}$).

Superconductivity characteristics of the samples were evaluated on the bases of magnetic susceptibility and resistivity measurements, see Figs. 3a and b, respectively. The most reduced samples of TCOD-400 and TCOD-500 were not superconductive. For all other samples bulk superconductivity was confirmed. The T_c values together with the superconducting volume fractions (as calculated from ZFC data at 5 K) are given in Table 1. In the $\rho - T$ curve (Fig. 3b), a sharp drop was observed for every superconductive sample, at a temperature that is very close to the T_c value determined on the basis of the $\chi - T$ data. However, zero-resistivity was not achieved for any of the HPO samples. This is a rather common phenomenon for samples high-pressure oxygenated using Ag_2O_2 as the oxygen source and it is attributed to the apparent existence of partly amorphous decomposition residue(s) of Ag_2O_2 at the boundaries of superconductive grains [15]. The same explanation is also valid to rationalize the somewhat high normal-state ρ values of the HPO samples. Moreover, in the $\chi - T$ curve a two-step transition was seen for the HPO samples (Fig. 3a). This may be considered as an indication that oxygen incorporation upon high-pressure oxygenation has not been perfectly homogeneous thorough the sample volume. For the AS sample synthesized in 1 atm O_2, T_c was found at 25 K, being in good agreement with the value originally reported by Sawa et al. [7]. Upon loading the phase with increasing amounts of oxygen T_c increased up to 62 K for the HPO:50 and HPO:100 samples (Table 1). The fact that the highest T_c value achieved was not due to the HPO samples being prepared with the largest amounts of Ag_2O_2 suggests that these samples (HPO:150 and HPO:200) might be (slightly) overdoped. In the following we discuss this on the basis of Cu $L_{2,3}$-edge XANES data for the hole-doping level of the samples.

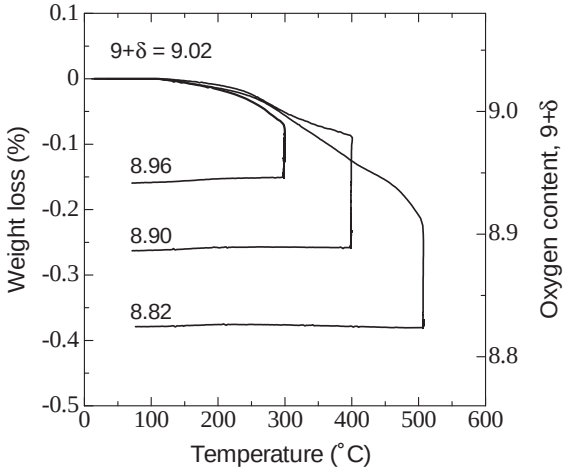

Fig. 2. TCOD curves for post-annealings carried out in N_2 gas for an AS sample of $Cu(Ba_{0.67}Eu_{0.33})_2(Ce_{0.33}Eu_{0.67})_2Cu_2O_{9\pm\delta}$ ($9\pm\delta = 9.02$) to obtain the oxygen-depleted samples of $9\pm\delta = 8.96$ (TCOD-300), 8.90 (TCOD-400) and 8.82 (TCOD-500). The given oxygen contents are from iodometric titrations.

The Cu $L_{2,3}$-edge XANES spectra (collected for most of the samples) are shown in Fig. 4. For the HPO samples, the Cu L_3-edge area of the spectra exhibits two readily distinguishable but overlapping peaks about 931.2 and 932.7 eV, due to nominally divalent (Cu^{II}: $3d^9$)

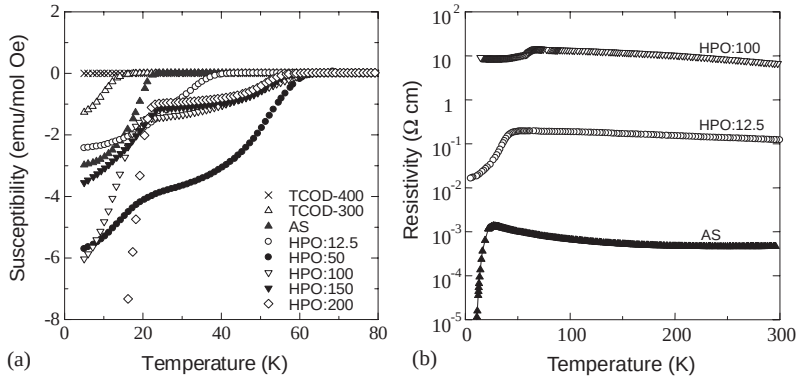

Fig. 3. Temperature dependence of: (a) magnetic susceptibility (ZFC), and (b) resistivity for selected $Cu(Ba_{0.67}Eu_{0.33})_2(Ce_{0.33}Eu_{0.67})_2Cu_2O_{9\pm\delta}$ samples.

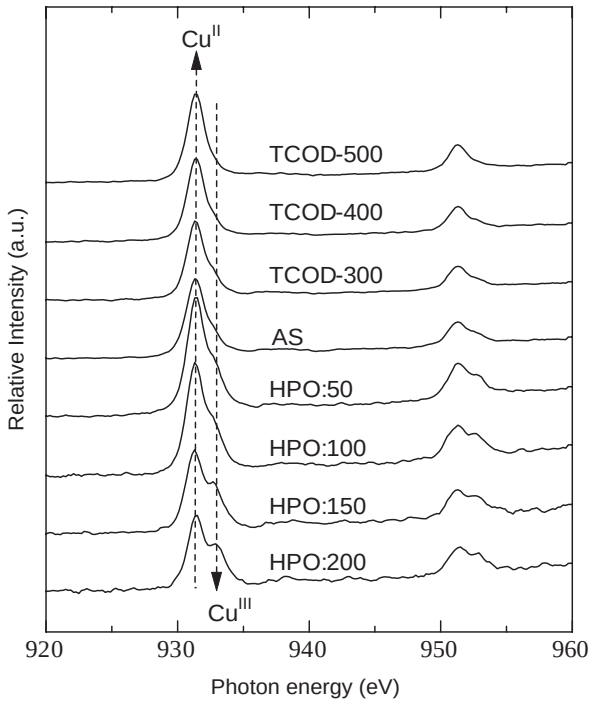

Fig. 4. Cu $L_{2,3}$-edge XANES spectra for the AS, TCOD and HPO samples of $Cu(Ba_{0.67}Eu_{0.33})_2(Ce_{0.33}Eu_{0.67})_2Cu_2O_{9\pm\delta}$: contributions from nominally divalent (Cu^{II}: $3d^9$) and trivalent (Cu^{III}: $3d^9L$) copper states are indicated.

and trivalent (Cu^{III}: $3d^9L$, where L = oxygen-ligand hole) copper states, respectively [24–26]. With decreasing oxygen content, i.e., going from the HPO samples to AS and TCOD samples, the intensity of the higher-energy peak due to Cu^{III} gradually decreases as a manifestation of the gradual decrease in the overall hole-doping level of the phase. At the same time, no sign of an additional peak around 934 eV is seen that would indicate the presence of (two-fold coordinated) monovalent Cu species. (Note that such a feature is clearly observed for oxygen-deficient samples of the Cu-1212 [26,27] and $(Pb_{2/3}Cu_{1/3})$-3212 [28] superconductors and also for the binary copper oxide Cu_2O [29], all containing monovalent Cu in a linear coordination.) We analyzed the Cu L_3-edge spectral features by fitting the intensities of the 931.2 and 932.7-eV peaks into a combination of Lorentzian and Gaussian functions after approximating the background to a straight line. The normalized integrated cross-section of the higher-energy peak, i.e., $I_{932.7}/(I_{931.2}+I_{932.7})$, should reflect (at least qualitatively) the extend of hole doping in the CuO_2 planes and the $CuO_{1\pm\delta}$ charge reservoir in average [24–27]. For the sake of an easier imagination, we convert this normalized intensity into an expression, $V(Cu)_{XAS} \equiv 2 + I_{932.7}/(I_{931.2}+I_{932.7})$, to get a number, that should be comparable to the chemical quantity of "average nominal valence state of copper" [30,31]. The resultant $V(Cu)_{XAS}$ values are listed in Table 1. From Table 1, it is seen that $V(Cu)_{XAS}$ increases monotonically from 2.04 for the TCOD-500 sample up to 2.33 for the HPO:200 sample. Among the TCOD and AS samples, comparison between the $V(Cu)_{XAS}$ and $V(Cu)_{tit}$ values reveals that the former values are systematically somewhat smaller than the latter ones, but the trends are consistent (Table 1). The small systematic difference in the absolute values of $V(Cu)_{XAS}$ and $V(Cu)_{tit}$ may originate from (i) the small CeO_2 impurity present in the samples (with a constant concentration), (ii) a possible systematic mistake in the fitting procedure of the spectral features, and/or (iii) anomalous transfer of spectral weight highly possible in strongly correlated systems [32]. In Fig. 5 we use the $V(Cu)_{XAS}$ values to show the relation between T_c and the overall hole-doping level for our Cu-1222 phase $Cu(Ba_{0.67}Eu_{0.33})_2(Ce_{0.33}Eu_{0.67})_2Cu_2O_{9\pm\delta}$ samples. With increasing $V(Cu)_{XAS}$ the phase becomes superconductive for $V(Cu)_{XAS} \geqslant 2.1$ and exhibits the highest T_c value of 62 K at $V(Cu)_{XAS} \approx 2.2$. With a further increase in $V(Cu)_{XAS}$, T_c slightly decreases presumably due to overdoping.

In comparison to the $V(Cu)_{XAS}$ values obtained for optimally doped samples of the Cu-1212 phase, i.e., $V(Cu)_{XAS} \approx V(Cu)_{tit} \approx 2.3$ in $CuBa_2YCu_2O_{6.93}$ [33], the present $V(Cu)_{XAS}$ value of ~2.2 for the optimally doped samples of the Cu-1222 phase looks somewhat low. As a possible explanation we suggest that in the two phases the excess positive charge may be differently distributed between the CuO_2 plane and the $CuO_{1\pm\delta}$ charge reservoir. Since the Cu L-edge XANES data do not allow us to differentiate the two types of copper–oxygen layers, we employed O K-edge XANES spectroscopy to obtain an estimate for the distribution of holes among

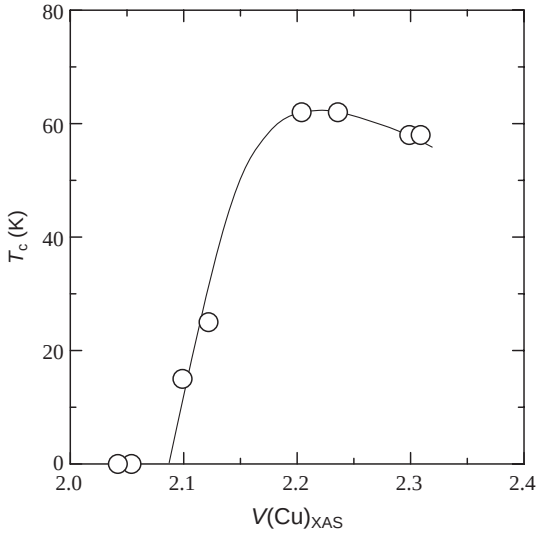

Fig. 5. T_c versus $V(Cu)_{XAS}$ (see the text for definition) for the variously oxygenated and deoxygenated Cu-1222-phase samples of $Cu(Ba_{0.67}Eu_{0.33})_2(Ce_{0.33}Eu_{0.67})_2Cu_2O_{9\pm\delta}$.

the different oxygen sites. In Fig. 6, O *K*-edge XANES spectra for the AS and TCOD samples in the energy range of 525–555 eV are displayed. (In the case of the HPO samples, O *K*-edge data were not considered due to Ag oxide inclusions in these samples in not well-defined amounts.) The pre-edge peak seen for all the samples about ~528.1 eV is the well-known signature of hole states in the *p*-type doped CuO_2 planes in high-T_c superconductors [20,25–28,31,34–36]. We can distinguish another pre-edge peak at ~527.3 eV partly overlapping with this peak. Taking analogy to the Cu-1212 phase [26,27,34,35], we assign this lower-energy pre-edge peak to the hole states in the $CuO_{1\pm\delta}$ charge reservoir. From Fig. 6, it is clearly seen that with increasing oxygen content the overall spectral weight below ~529 eV increases as expected. Another indication of the increasing hole-doping level is the shift of the "528.1-eV peak" to slightly lower absorption energies; in other words, the Fermi level moves to a lower energy when the hole concentration within the CuO_2 plane increases. In order to get quantitative information on the hole distribution between the CuO_2 plane and the $CuO_{1\pm\delta}$ charge reservoir, we fitted the pre-edge peaks with Gaussian functions. The background was approximated by a straight line. Thus-obtained values of spectral weight (in MbeV per unit cell) for the 527.3- and 528.1-eV peaks were then "standardized" against the value of 15 MbeV that corresponds to one hole in the Cu-1212 phase [26,34] to get rough estimates for the absolute hole numbers in one $CuO_{1\pm\delta}$ charge-reservoir unit [$p(CuO_{1\pm\delta})_{XAS}$] and two CuO_2-plane units [$2p(CuO_2)_{XAS}$], respectively. (Note that the spectral weight due to the CuO_2-plane hole states corresponds to two copper–oxygen planes, whereas that of the $CuO_{1\pm\delta}$ charge reservoir corresponds to one copper–oxygen layer only.) The resultant layer-specific hole concentrations, $p(CuO_{1\pm\delta})_{XAS}$ and $p(CuO_2)_{XAS}$, are given in Table 1. Obviously, in our Cu-1222 phase samples of $Cu(Ba_{0.67}Eu_{0.33})_2(Ce_{0.33}Eu_{0.67})_2Cu_2O_{9\pm\delta}$ the CuO_2 plane is more heavily doped with holes than the $CuO_{1\pm\delta}$ charge reservoir, whereas the opposite is true in fully oxygenated samples of the Cu-1212 phase [9,26,27,33–35]. Hence, the CuO_2-plane hole concentration in optimally doped Cu-1222 (with presumably somewhat lower overall hole-doping level) may not be much different from that in optimally doped Cu-1212.

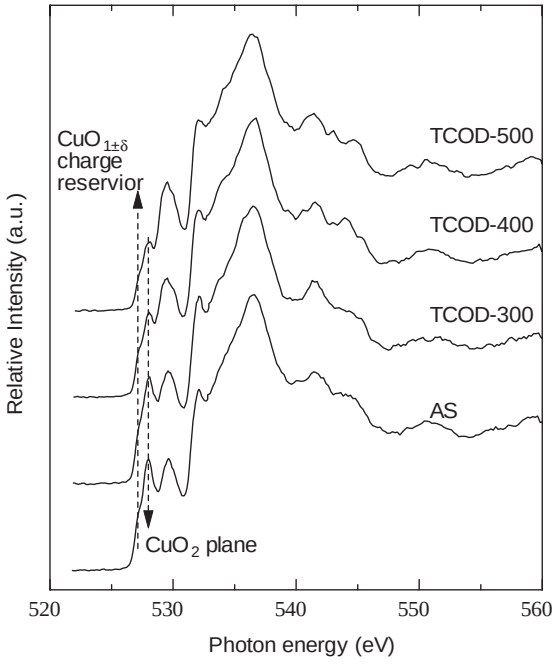

Fig. 6. O *K*-edge XANES spectra for the AS and TCOD samples of $Cu(Ba_{0.67}Eu_{0.33})_2(Ce_{0.33}Eu_{0.67})_2Cu_2O_{9\pm\delta}$: contributions from the CuO_2 plane and $CuO_{1\pm\delta}$ charge reservoir hole states are indicated. (Note that the spectral weight due to the CuO_2 plane hole states corresponds to two copper–oxygen planes, whereas that of the $CuO_{1\pm\delta}$ charge reservoir corresponds to one copper–oxygen layer only.)

4. Conclusions

The Cu-1222 phase was found flexible enough for wide-range oxygen-content tuning. By means of a set of deoxygenation (in N_2) and oxygenation (under high O_2 pressures) annealing treatments the hole-doping level of the phase could be continuously adjusted from a nondoped (nonsuperconductive) state to a slightly overdoped state. For optimally doped samples T_c reached a value as high as 62 K. From Cu *L*-edge XANES spectroscopy data the overall hole-doping level looked somewhat low in comparison to optimally doped samples of the Cu-1212 phase. However, O *K*-edge XANES data revealed that in Cu-1222 [at least with the cation stoichiometry of $Cu(Ba_{0.67}Eu_{0.33})_2(Ce_{0.33}Eu_{0.67})_2Cu_2O_{9\pm\delta}$] the holes are more efficiently accommodated by the CuO_2 plane than in the Cu-1212 phase.

Acknowledgment

This work was supported by Grants-in-aid for Scientific Research (Nos. 15206002 and 15206071) from the Japan Society for the Promotion of Science.

References

[1] J. Akimitsu, S. Suzuki, M. Watanabe, H. Sawa, Jpn. J. Appl. Phys. 27 (1988) L1859.
[2] H. Sawa, S. Suzuki, M. Watanabe, J. Akimitsu, H. Matsubara, H. Watabe, S. Uchida, K. Kokusho, H. Asano, F. Izumi, E. Takayama-Muromachi, Nature 337 (1989) 347.
[3] J.M. Longo, P.M. Raccah, J. Solid State Chem. 6 (1973) 526.
[4] B. Grande, H. Müller-Buschbaum, M. Schweizer, Z. Anorg, Allg. Chem. 428 (1977) 120.
[5] Hk. Müller-Buschbaum, W. Wollschlaeger, Z. Anorg, Allg. Chem. 414 (1975) 76.

[6] Y. Tokura, H. Takagi, S. Uchida, Nature 337 (1989) 345.
[7] H. Sawa, K. Obara, J. Akimitsu, Y. Matsui, S. Horiuchi, J. Phys. Soc. Japan 58 (1989) 2252.
[8] The T, T^* and T structures are denoted as 0201 (Category-A), 0222 and 0021 (Category-B), respectively.
[9] M. Karppinen, H. Yamauchi, Mater. Sci. Eng. R 26 (1999) 51.
[10] T. Wada, A. Ichinose, H. Yamauchi, S. Tanaka, J. Ceram. Soc. Jpn. Int. Ed. 99 (1991) 420.
[11] M. Marezio, E.V. Antipov, J.J. Capponi, C. Chaillout, S. Loureiro, S.N. Putilin, A. Santoro, J.L. Tholence, Physica B 197 (1994) 570.
[12] A group of phases with the $[A\mathrm{O}]$-$[(M\mathrm{O}_{1\pm\delta/m})_m]$-$[A\mathrm{O}]$ "blocking block" fixed but the number, s, of the fluorite-structured cation layers varying form a homologous series of Category-B.
[13] H. Yamauchi, M. Karppinen, S. Tanaka, Physica C 263 (1996) 146.
[14] M.K. Wu, J.R. Ashburn, C.J. Torng, P.H. Hor, R.L. Meng, L. Gao, Z.J. Huang, Y.Q. Wang, C.W. Chu, Phys. Rev. Lett. 58 (1987) 908.
[15] Y. Morita, T. Nagai, Y. Matsui, H. Yamauchi, M. Karppinen, Phys. Rev. B 70 (2004) 174515.
[16] A. Ono, Jpn. J. Appl. Phys. 32 (1993) 4517.
[17] A. Ono, Jpn. J. Appl. Phys. 32 (1993) L1599.
[18] M. Karppinen, H. Yamauchi, Oxygen engineering for functional oxide materials, in: A.V. Narlikar (Ed.), International Book Series: Studies of High Temperature Superconductors, Vol. 37, Nova Science Publishers, New York, 2001, pp. 109–143.
[19] M. Karppinen, A. Fukuoka, L. Niinistö, H. Yamauchi, Supercond. Sci. Technol. 9 (1996) 121.
[20] M. Karppinen, H. Yamauchi, Y. Morita, M. Kitabatake, T. Motohashi, R.S. Liu, J.M. Lee, J.M. Chen, J. Solid State Chem. 177 (2004) 1037.
[21] M. Karppinen, V.P.S. Awana, Y. Morita, H. Yamauchi, Physica C 392–396 (2003) 82.
[22] F. Izumi, E. Takayama-Muromachi, M. Kobayashi, Y. Uchida, H. Asano, T. Ishigaki, N. Watanabe, Jpn. J. Appl. Phys. 27 (1988) L824.
[23] E. Goodilin, M. Limonov, A. Panfilov, N. Khasanova, A. Oka, S. Tajima, Y. Shiohara, Physica C 300 (1998) 250.
[24] D.D. Sarma, O. Strebel, C.T. Simmons, U. Neukirch, G. Kaindl, R. Hoppe, H.P. Müller, Phys. Rev. B 37 (1988) 9784.
[25] A. Bianconi, M. DeSantis, A. Di Ciccio, A.M. Flank, A. Fronk, A. Fontaine, P. Legarde, H.K. Yoshida, A. Kotani, A. Marcelli, Phys. Rev. B 38 (1988) 7196.
[26] N. Nücker, E. Pellegrin, P. Schweiss, J. Fink, S.L. Molodtsov, C.T. Simmons, G. Kaindl, W. Frentrup, A. Erb, G. Müller-Vogt, Phys. Rev. B 51 (1995) 8529.
[27] M. Karppinen, H. Yamauchi, T. Nakane, K. Fujinami, K. Lehmus, P. Nachimuthu, R.S. Liu, J.M. Chen, J. Solid State Chem. 166 (2002) 229.
[28] M. Karppinen, M. Kotiranta, H. Yamauchi, P. Nachimuthu, R.S. Liu, J.M. Chen, Phys. Rev. B 63 (2001) 184507.
[29] [a] M. Grioni, J.B. Goedkoop, R. Schoorl, F.M.F. de Groot, J.C. Fuggle, F. Schäfers, E.E. Koch, G. Rossi, J.-M. Esteva, R.C. Karnatak, Phys. Rev. B 39 (1989) 1541;
[b] M. Grioni, J.F. van Acker, M.T. Czyżyk, J.C. Fuggle, Phys. Rev. B 45 (1992) 3309.
[30] N. Merrien, F. Studer, G. Poullain, C. Michel, A.M. Flank, P. Lagarde, A. Fontaine, J. Solid State Chem. 105 (1993) 112.
[31] M. Karppinen, K. Kotiranta, T. Nakane, S.C. Chang, J.M. Chen, R.S. Liu, H. Yamauchi, Phys. Rev. B 67 (2003) 134522.
[32] M.A. van Veenendaal, G.A. Sawatzky, Phys. Rev. B 49 (1994) 3473.
[33] We synthesized a $CuBa_2YCu_2O_{6.93}$ reference sample and characterized it for $V(\mathrm{Cu})_{\mathrm{XAS}}$ (≈ 2.3) and T_c ($= 93\,\mathrm{K}$) through procedures equivalent to those used for the present samples.
[34] A. Krol, Z.H. Ming, Y.H. Kao, N. Nücker, G. Roth, J. Fink, G.C. Smith, K.T. Park, J. Yu, A.J. Freeman, A. Erband, G. Müller-Vogt, J. Karpinski, E. Kaldis, K. Schönmann, Phys. Rev. B 45 (1992) 2581.
[35] M. Merz, N. Nücker, P. Schweiss, S. Schuppler, C.T. Chen, V. Chakarian, J. Freeland, Y.U. Idzerda, M. Kläser, G. Müller-Vogt, Th. Wolf, Phys. Rev. Lett. 80 (1998) 5192.
[36] E. Pellegrin, J. Fink, C.T. Chen, Q. Xiong, Q.M. Lin, C.W. Chu, Phys. Rev. B 53 (1996) 2767.